BEM for modeling fracture mechanics problems

Andrés Sáez

University of Seville (Spain)

Collaborators: J. Domínguez, Ch. Zhang, F. García-Sánchez, R. Rojas-Díaz, M. Wünsche

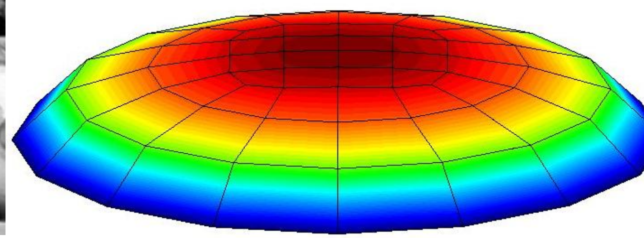

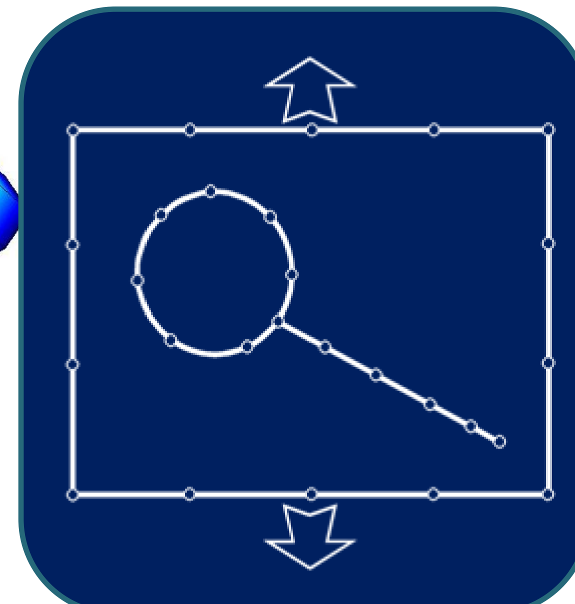

NSF Workshop on the Emerging Applications and Future Directions of the Boundary Element Method

September 1-3, 2010

Cleveland, Ohio, USA (The University of Akron Campus)

Motivation:
Structural Integrity of Advanced Materials

Design of structural materials demands for high performance applications: we want lighter materials and new capacities

- Tailored materials with good strength/weight ratio → composites
- Multifield materials for control and smart structures applications → piezoelectricity…

Damage Tolerance Philosophy

- Existence of a flaw (crack…) in a mechanical component will no imply the end of its service life → need to evaluate its performance and reliability

Motivation:
Structural Integrity of Advanced Materials

Tools to clearly characterize how a damaged structural element behaves are thus needed in order to predicts its:

- working conditions &
- remaining service life

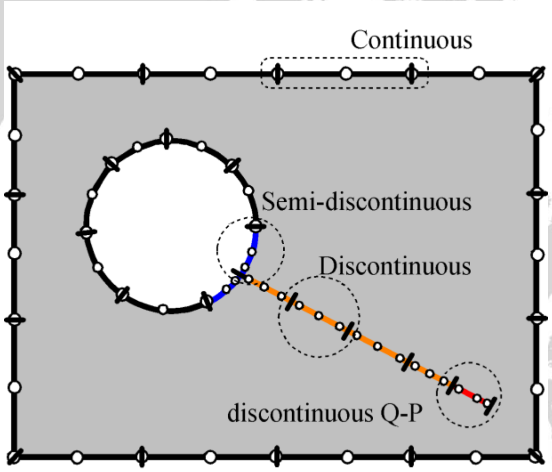

Structural Integrity of Advanced Materials

The AIM is to extend to this new class of materials the damage estimation techniques previously developed for *classic* materials

WE'LL TACKLE THE PROBLEM FROM A NUMERICAL POINT OF VIEW (BEM)

Outline

- Fracture mechanics of advanced materials:
  - Anisotropic materials (composites)
  - Multifield materials:
    - Piezoelectric
    - Magnetoelectroelastic
- Why BEM for fracture?
- BEM strategies for fracture mechanics
- Dual or Hypersingular BEM
  - Statics
  - Dynamics
- Concluding remarks

Fracture mechanics of anisotropic materials

- Anisotropic materials in nature: Zinc, magnesium, wood, ice…
- Engineered materials: composites

2-D anisotropic behavior law

$$\begin{Bmatrix} \varepsilon_{11} \\ \varepsilon_{22} \\ 2\varepsilon_{12} \end{Bmatrix} = \begin{pmatrix} a_{11} & a_{12} & a_{16} \\ a_{12} & a_{22} & a_{26} \\ a_{16} & a_{26} & a_{66} \end{pmatrix} \begin{Bmatrix} \sigma_{11} \\ \sigma_{22} \\ \sigma_{12} \end{Bmatrix}$$

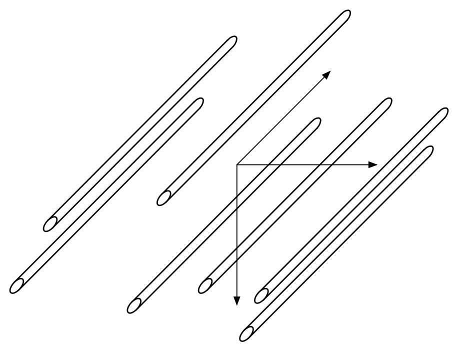

The existence of a crack will alter the stress fields and may lead to failure for loads much lower than the design load bearing capacity of the component

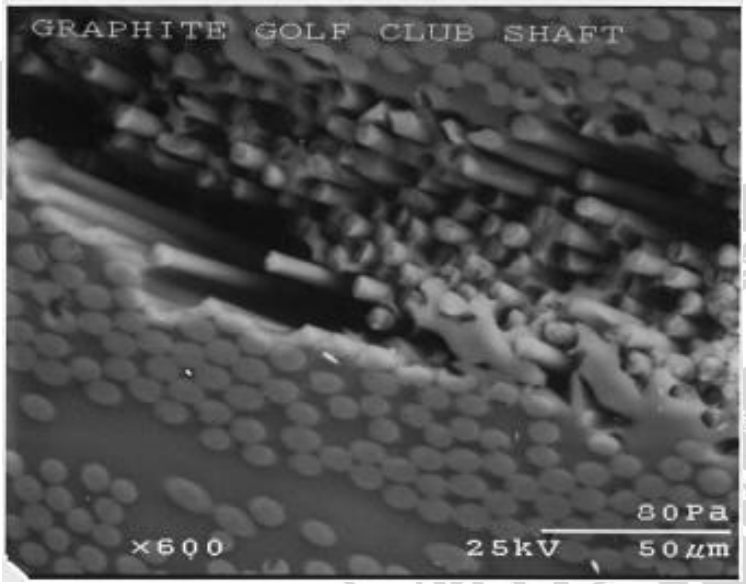

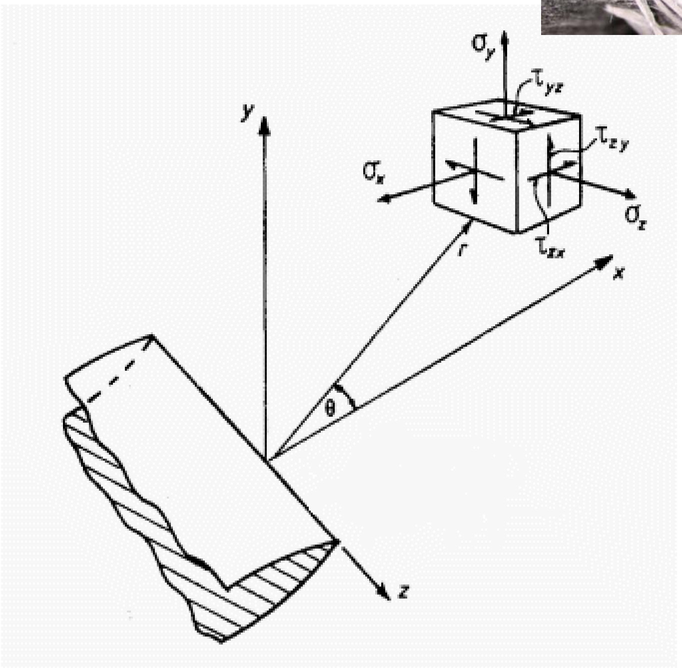

- MICRO-scale
- MESO-scale
- MACRO-scale ← This talk

Displacement and stress fields around the crack tip[1]:

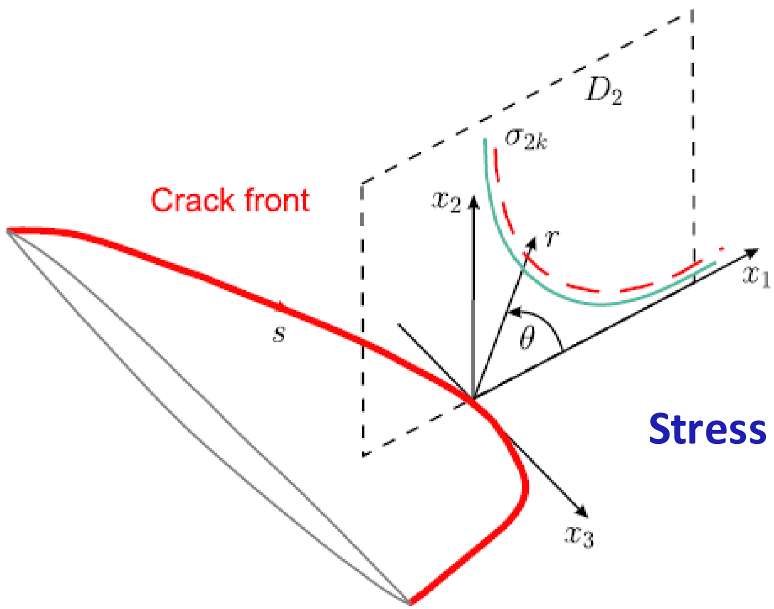

$$\sigma = K\, f(\theta, C_{ij}) / \sqrt{r}$$

$$u = K\, g(\theta, C_{ij}) \sqrt{r}$$

Stress Intensity Factors (SIF)

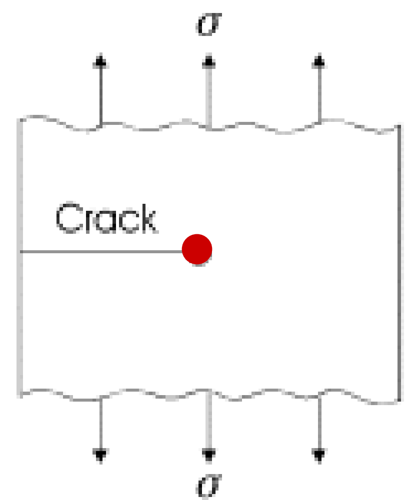

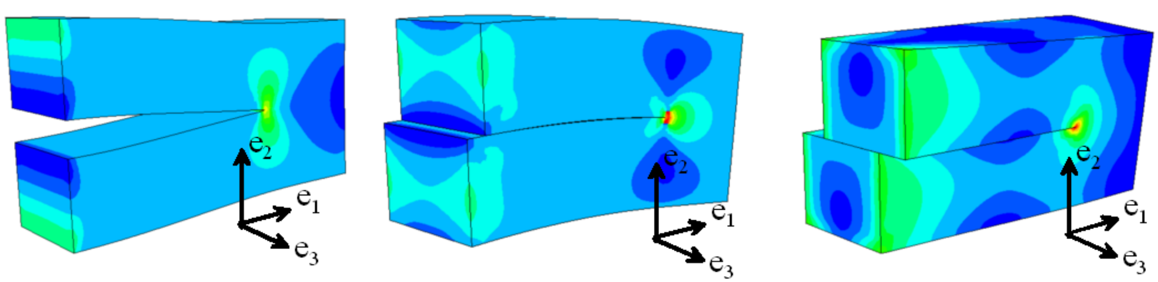

Mode I Mode II Mode III

(1) Sih, Paris e Irwin (1965)

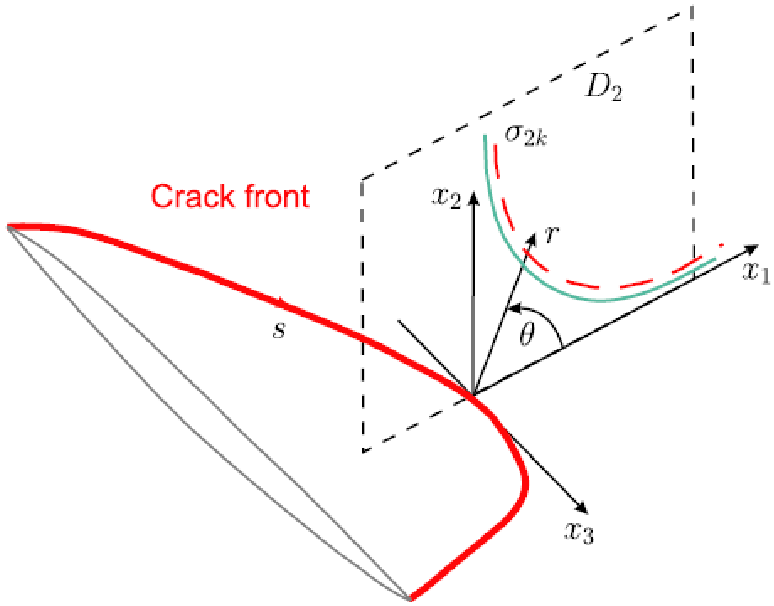

$$\sigma = K\, f(\theta, C_{ij}) / \sqrt{r}$$

$$u = K\, g(\theta, C_{ij}) \sqrt{r}$$

When tackling the problem numerically, the selected method should fulfill some requirements:

- Adequate representation of the mechanical fields around the crack
- SIF (or other fracture parameters) accurate computation
- Easy crack discretization

Fracture mechanics of multifield materials

Ability to convert energy among mechanical and non-mechanical fields:

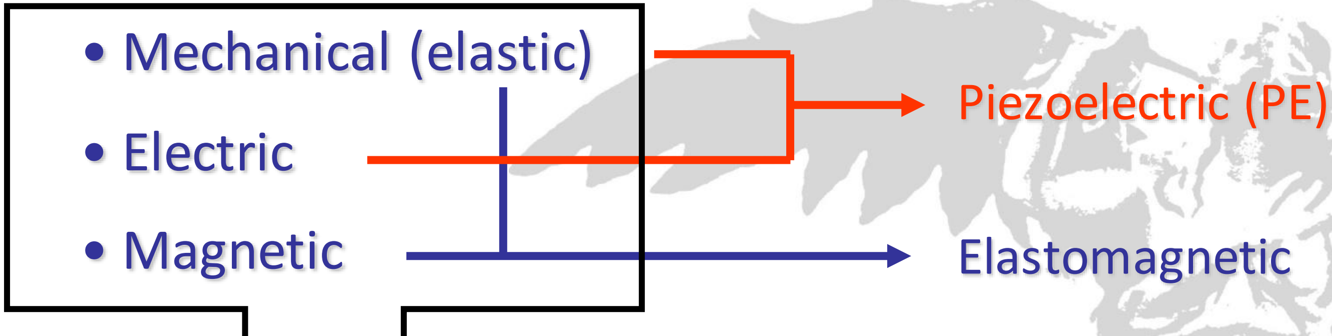

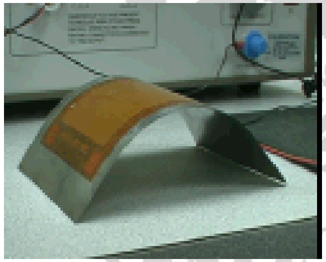

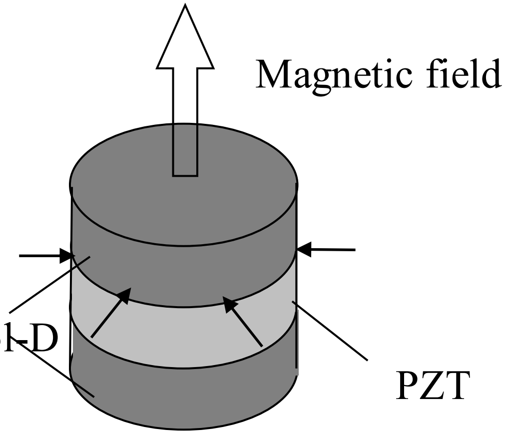

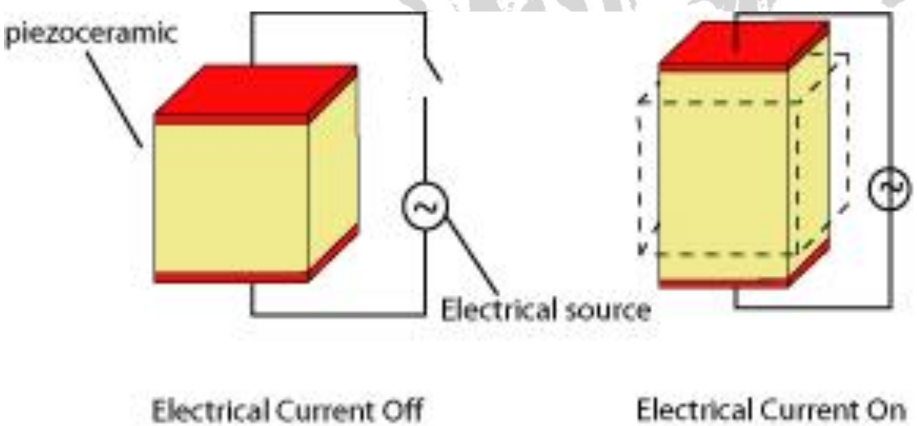

Piezoelectric Materiales

Direct piezoelectric effect [1]: a voltage is produced when the material is under tension or compression stress.

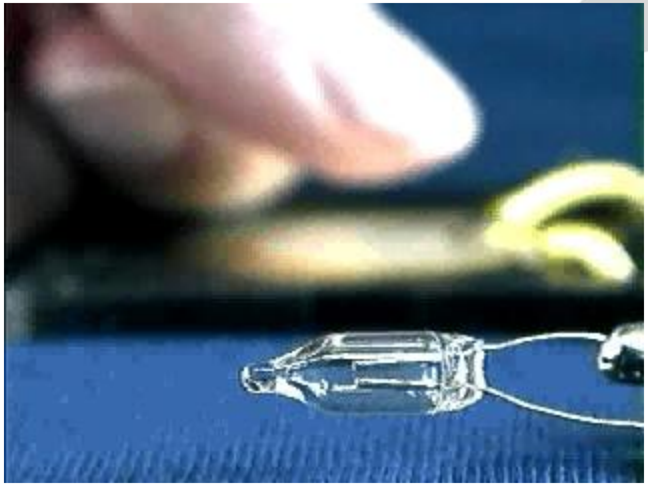

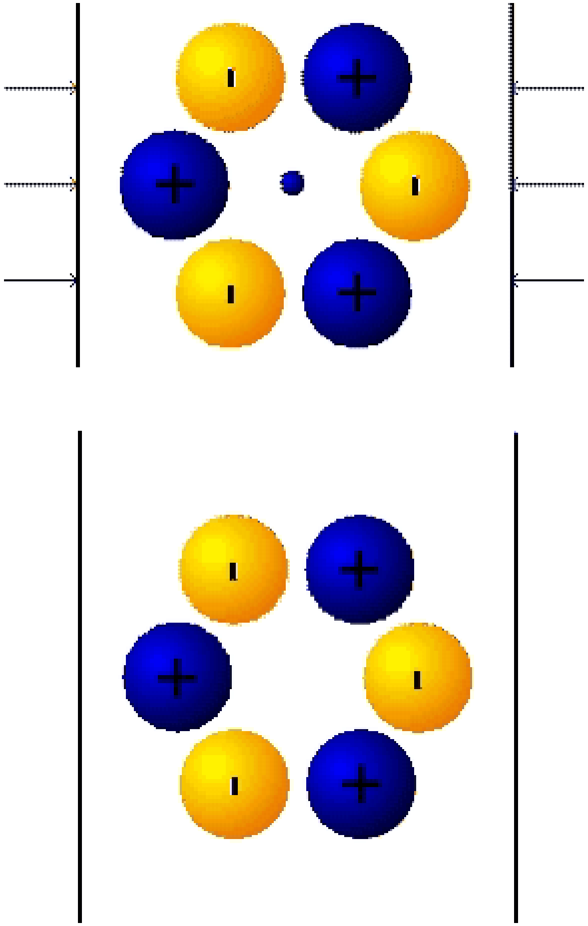

[1] Jacques y Pierre Curie, 1880

Inverse piezoelectric effect: when a potential difference is applied across the crystal it causes its deformation.

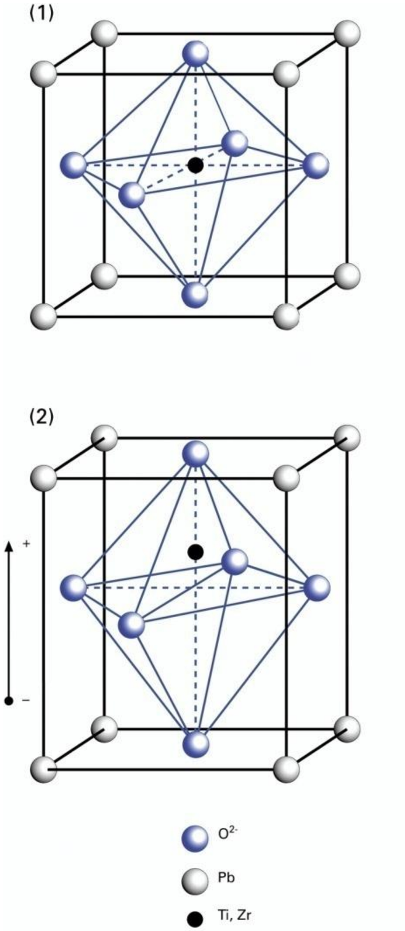

PZT unit cell:

1. PZT unit cell in the symmetric cubic state above the Curie temperature.
2. Tetragonally distorted unit cell below the Curie temperature.

PE materials

- Are always anisotropic
- Show larger PE coupling for artificial materials (e.g., PZT ceramics)

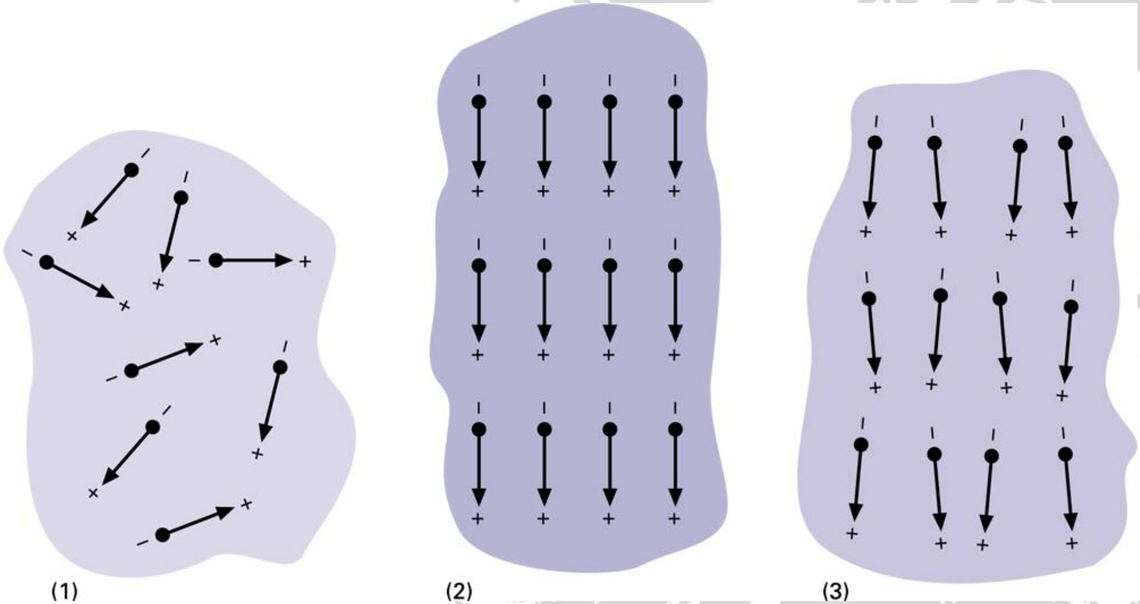

Electric dipoles in domains:

1. unpoled ferroelectric ceramic
2. during and
3. after poling (piezoelectric ceramic).

Applications for PE materials:

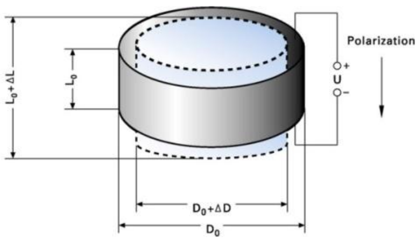

- sensors
- actuators

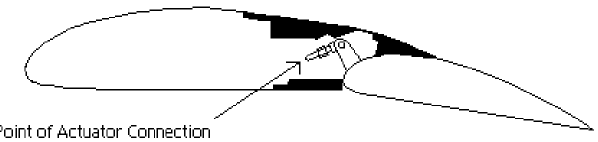

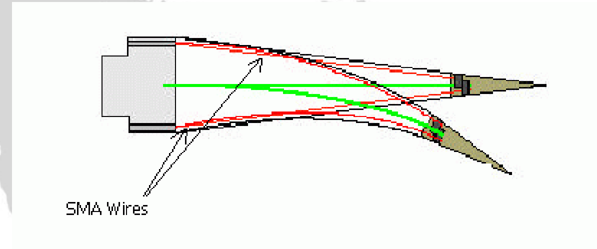

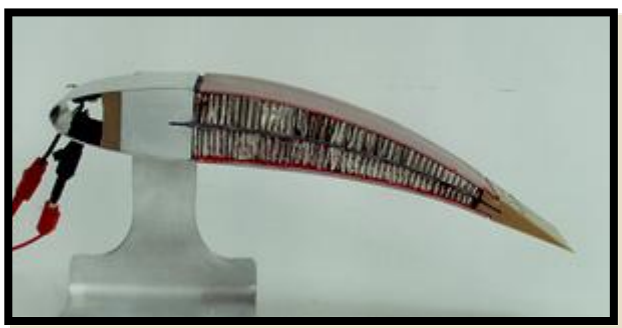

Applications for PE materials: Smart structures

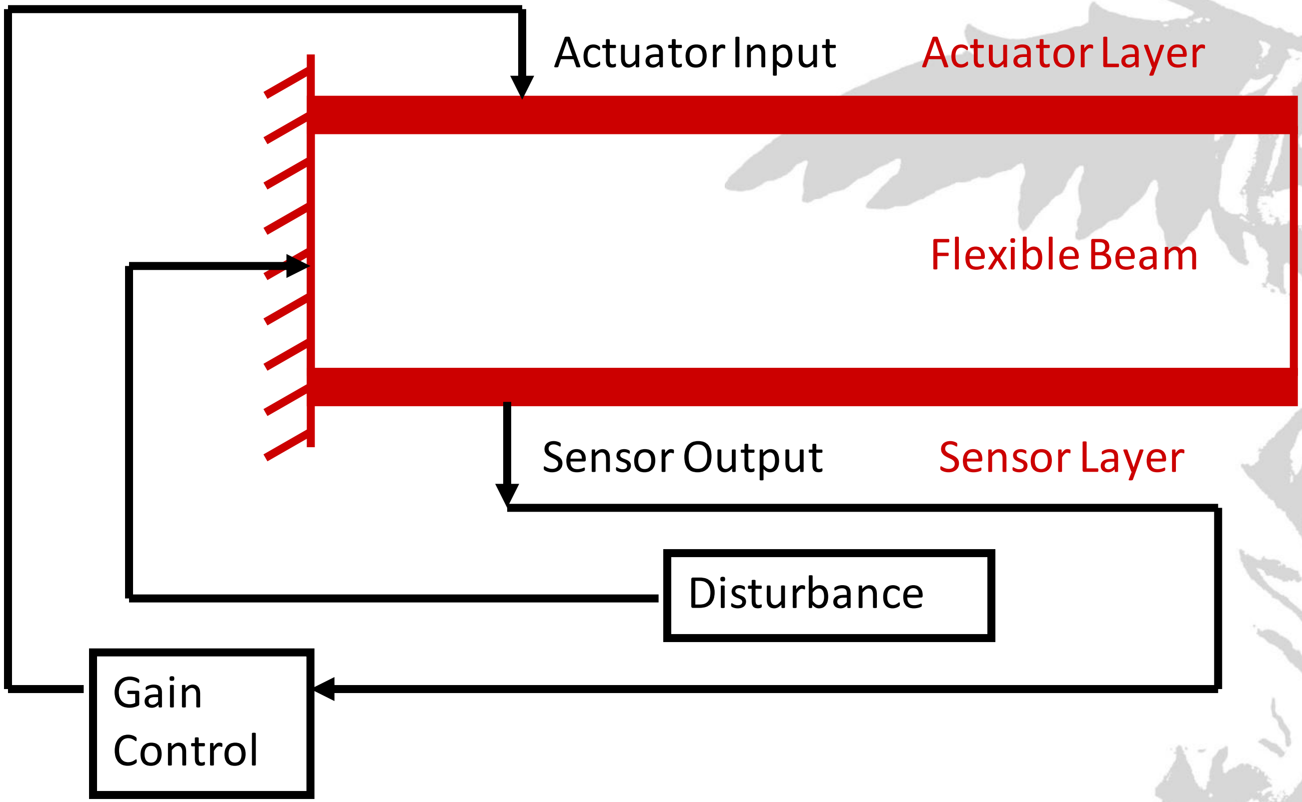

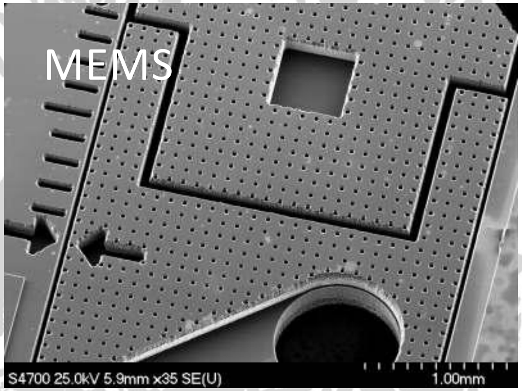

How do we model PE materials?:

Extended notation for piezoelectricity (Barnett & Lothe, 1975)

Extended displacements vector

$$u_I = \begin{cases} u_i & I = 1,2,3 \\ \varphi & I = 4 \end{cases}$$

Electric potential

Extended stress tensor

$$\sigma_{iJ} = \begin{cases} \sigma_{ij} & I = 1,2,3 \\ D_i & I = 4 \end{cases}$$

Electric displacement

PE behavior law

$$\begin{pmatrix} \sigma_{ij} \\ D_i \end{pmatrix} = \underbrace{\begin{pmatrix} C_{ijlm} & e_{kji} \\ e_{ijk} & -\kappa_{ij} \end{pmatrix}}_{C_{iJLm}} \begin{pmatrix} u_{l,m} + u_{m,l} \\ \varphi_{,j} \end{pmatrix}$$

$$\boxed{\sigma_{iJ,i} = 0}$$

C_{iJLm} elastic, piezoelectric & dielectric constants

Magnetoelectroelastic materials

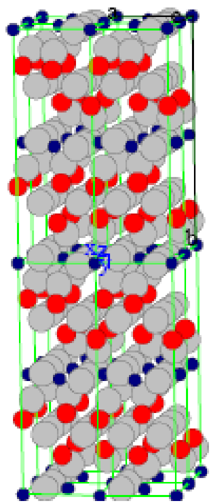

$YMnO_3$

$BiMnO_3$

Composite materials consisting of both piezoelectric and piezomagnetic phases may exhibit a magnetoelectric coupling effect that is not shown by any of the material phases alone. The magnetoelectric coupling of the resulting composite may be much larger that that of a single phase magnetoelectric material (Van Suchtelen, 1972; Nan, 1994; Benveniste, 1995).

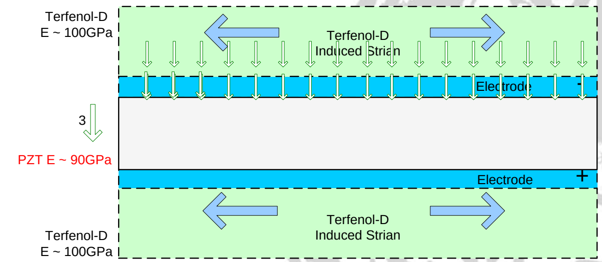

d_{31} mode

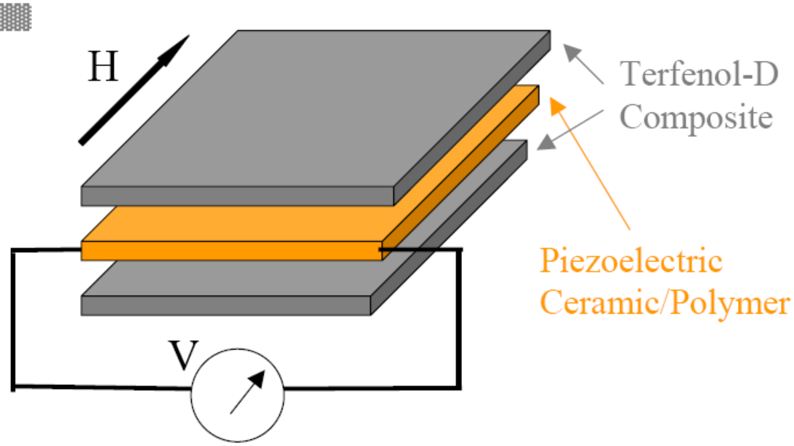

Conductive Epoxy

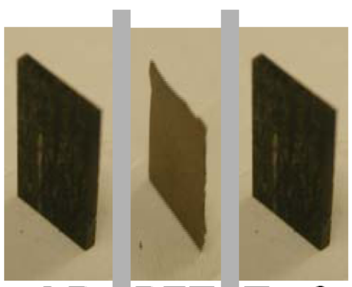

Terfenol-D Composite **PZT-5H** **Terfenol-D Composite**

Laminated [2-2] Magnetoelectric Composite

Modeling MEE materials

Magnetoelectroelastic materials may be formulated in an elastic-like fashion by using the following generalized notation:

Extended displacement vector

$$u_I = \begin{cases} u_i & I = 1,2,3 \\ \phi & I = 4 \\ \varphi & I = 5 \end{cases}$$

Extended stress tensor

$$\sigma_{iJ} = \begin{cases} \sigma_{ij} & I = 1,2,3 \\ D_i & I = 4 \\ B_i & I = 5 \end{cases}$$

Electric potential

Magnetic potential

Electric displacement

Magnetic induction

Constitutive equations: $\sigma_{iJ} = C_{iJKl} u_{K,l}$

Why study fracture in multifield materials?:

- **structural integrity**
- **cracks alter the electric/magnetic reading: may lead to adopt wrong decissions (the structure is no longer smart)**
- **the electric and magnetic fields have influence on the crack growth process**

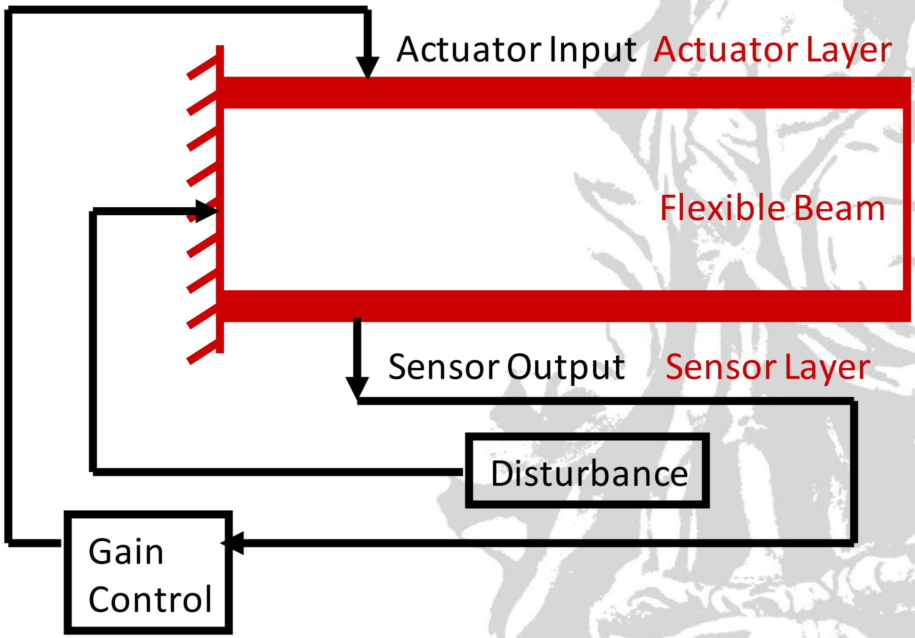

Fracture mechanics of multifield materials

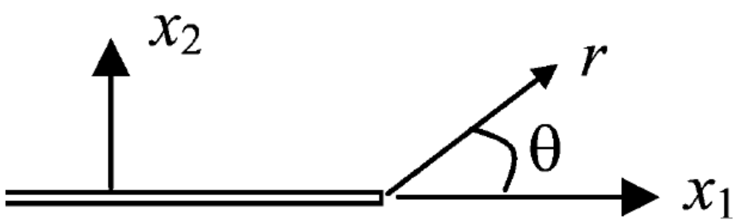

$$\sigma = \boxed{K}\, f(\theta, C_{ij}) / \sqrt{r}$$

$$u = \boxed{K}\, g(\theta, C_{ij}) \sqrt{r}$$

Generalized intensity factors:

- stress intensity factors (SIF): K_I and K_{II}
- electric displacement intensity factor (EDIF): K_D
- magnetic induction intensity factor (MIIF): K_B

Fracture of PE materials

Parton, V.Z., Fracture mechanics of piezoelectric materials, Acta Astronautica, 3 (1976), pp. 671-683.

Pak, Y.E., Crack extension force in a piezoelectric material, Journal of Applied Mechanics, Transactions ASME, 57 (1990), pp. 647-653.

Fracture of MEE materials

Song, Z.F., Sih, G.C., Crack initiation behavior in magnetoelectroelastic composite under in-plane deformation, Theor. and Appl. Fract. Mechanics, 39 (2003), pp. 189-207.

Wang, B.L., Mai, Y.-W., Crack tip field in piezoelectric/piezomagnetic media, European Journal of Mechanics, A/Solids, 22 (2003), pp. 591-602.

Why BEM for fracture?

Is BEM able to answer properly the questions we previously raised?

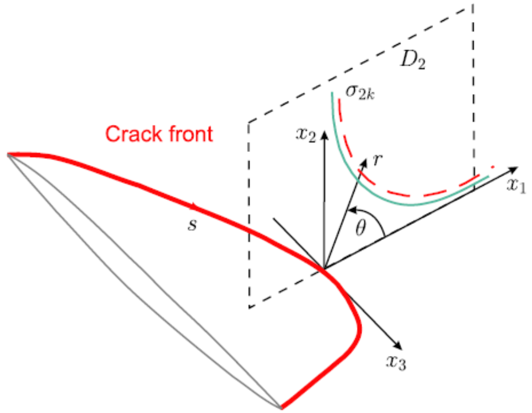

$$\sigma = K f(\theta, C_{ij}) / \sqrt{r}$$

$$u = K g(\theta, C_{ij}) \sqrt{r}$$

When tackling the problem numerically, the selected method should fulfill some requirements:

- Adequate representation of the field variables around the crack
- SIF (or other fracture parameters) accurate computation
- Easy crack discretization

The answer is YEAH !!!!

Some BEM advantages

- The mesh is reduced in one dimension
- Automatic satisfaction of the radiation conditions at infinity
- Ability to capture high stress gradients
- Easy implementation of elements modeling crack-tip fields in fracture

Some disadvantages

- Singular integrations
- (Need appropriate fundamental solution)

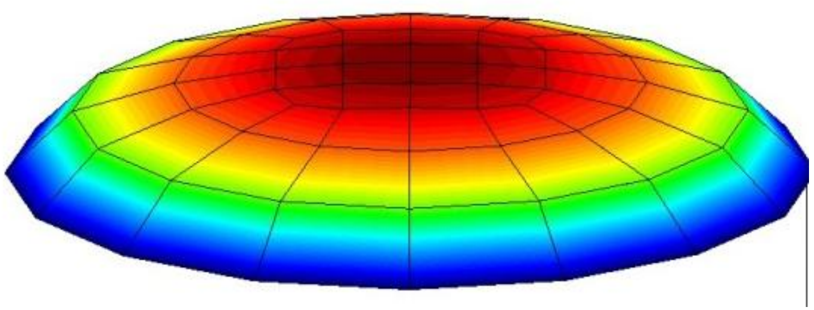

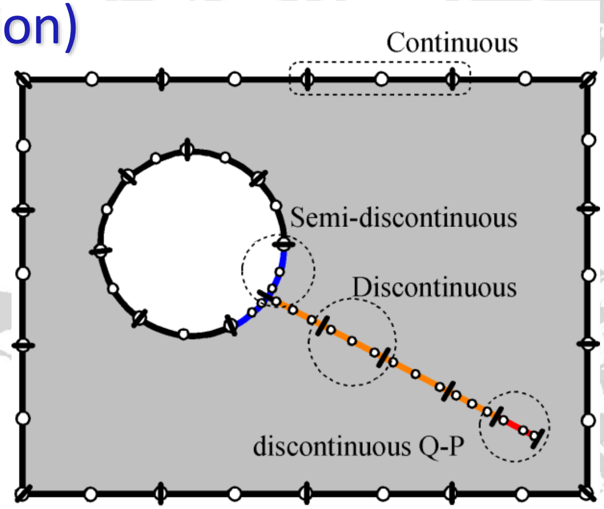

BEM strategies for fracture mechanics

$$c_{IJ}u_J(\xi)+\int_\Gamma p^*_{IJ}(\xi,x)u_J(x)d\Gamma(x)=\int_\Gamma u^*_{IJ}\,p_J\,d\Gamma$$

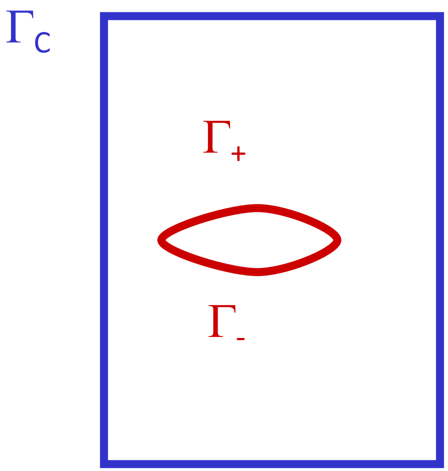

0. Use *tailored* fundamental solutions

1. Subregion technique

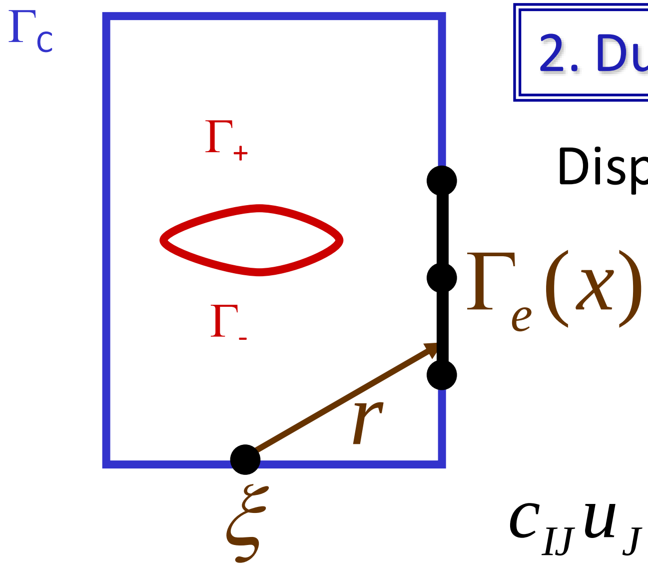

2. Dual or hypersingular BEM

Displacement Boundary Integral Equation (BIE)

ξ Collocation point

x Observation point

$$c_{IJ}u_J(\xi)+\int_\Gamma p_{IJ}^*(\xi,x)u_J(x)d\Gamma(x)=\int_\Gamma u_{IJ}^* p_J d\Gamma$$

$$\Big\downarrow N_r C_{iJLr}\frac{\partial}{\partial\xi}$$

Traction BIE

$$c_{IJ}p_J+N_r\int_\Gamma s_{rIJ}^* u_J d\Gamma = N_r\int_\Gamma d_{rIJ}^* p_J d\Gamma$$

$$u^*\propto\Theta(\ln r)\ \Rightarrow\ d^*\propto\Theta(1/r)$$

$$p^*\propto\Theta(1/r)\ \Rightarrow\ s^*\propto\Theta(1/r^2)$$

Extended C.O.D. Δu $\Delta\phi$ $\Delta\varphi$

$$\Delta p = 0$$

$$D = 0$$

$$B = 0$$

Dual or hypersingular BEM

$$c_{IJ}u_J(\xi) + \int_\Gamma p^*_{IJ}(\xi, x)u_J(x)d\Gamma(x) = \int_\Gamma u^*_{IJ} p_J d\Gamma$$

$$c_{IJ} p_J + N_r \int_\Gamma s^*_{rIJ} u_J d\Gamma = N_r \int_\Gamma d^*_{rIJ} p_J d\Gamma$$

- Meshing strategy?
- Availability of reasonable fundamental solutions for statics?
- Singular and hypersingular integrations?
- Computation of fracture parameters?
- What about dynamics?

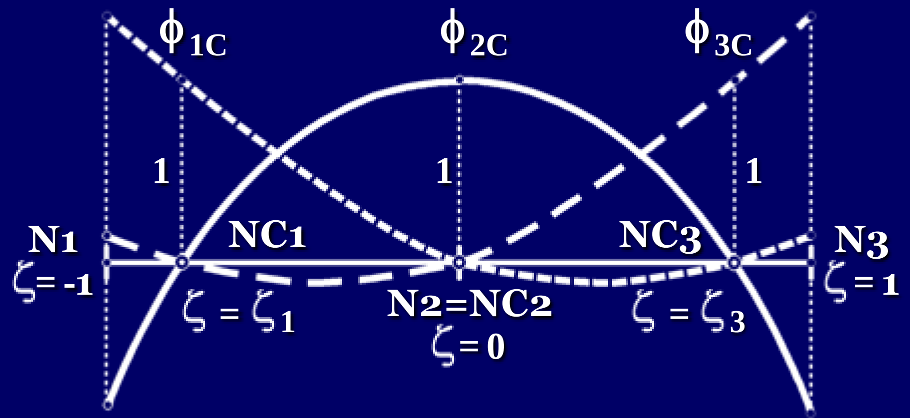

Meshing strategy

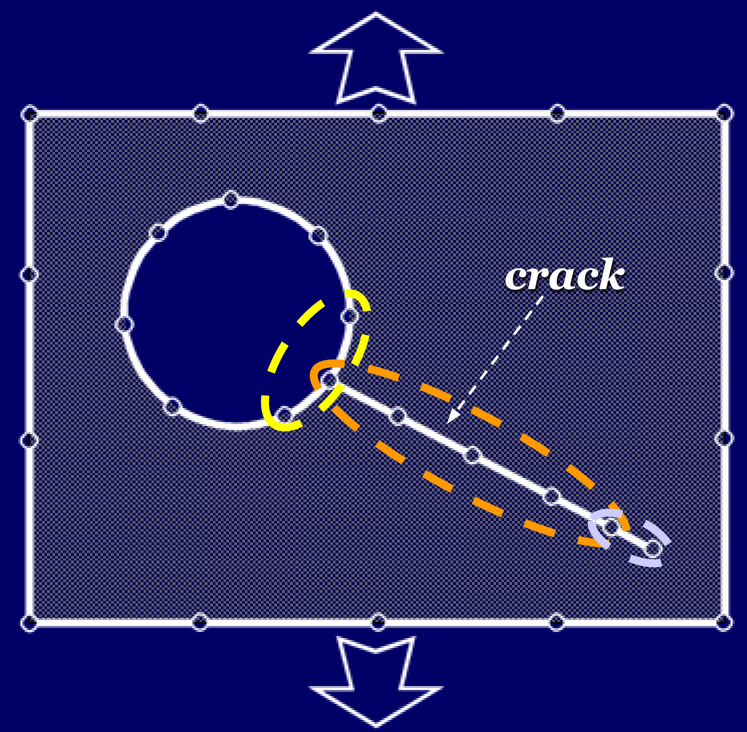

continuous DBIE (Γc)

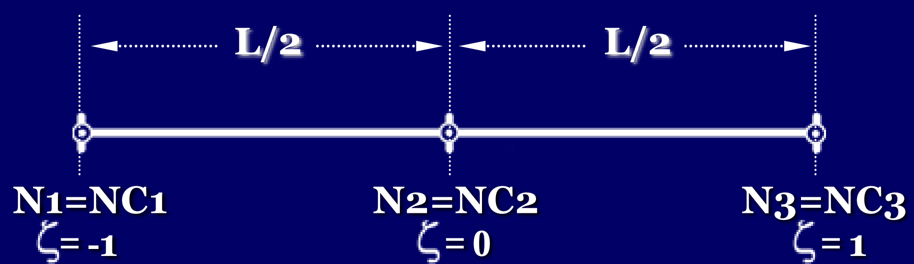

Traction BIE (TBIE) $\longrightarrow$ *displacement field* C^1

discontinuous TBIE $(\Gamma +)$

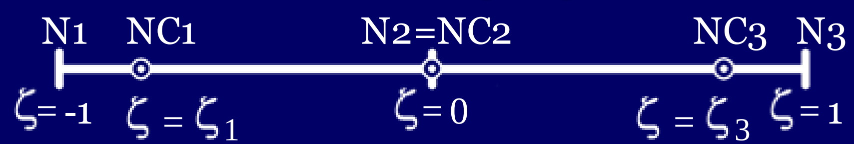

semidiscontinuous EID (Γc)

discontinuous quarter-point $(\Gamma +)$

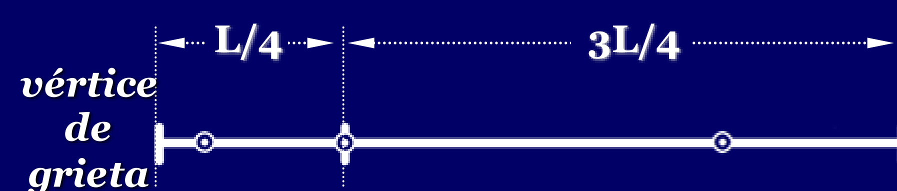

Static fundamental solution

$$u_{IJ}^{*S} = \mathrm{Re}\left[\sum_{R=1}^{5} A_{JR} H_{RI} \boxed{\ln(z_R^x - z_R^\xi)}\right] \longrightarrow d_{IJ}^{*S} = d_{rIJ}^{*S} N_r \propto \mathrm{Re}\left[\boxed{\frac{\mu_R N_1 - N_2}{(z_R^x - z_R^\xi)}}\right]$$

$$p_{IJ}^{*S} = \mathrm{Re}\left[\sum_{R=1}^{5} L_{JR} H_{RI} \boxed{\frac{\mu_R n_1 - n_2}{(z_R^x - z_R^\xi)}}\right] \longrightarrow s_{rIJ}^{*S} \propto \mathrm{Re}\left[\boxed{\frac{\mu_R n_1 - n_2}{(z_R^x - z_R^\xi)^2}}\right]$$

Observation point ξ: $\quad z_R^\xi = \xi_1 + \mu_R \xi_2 \quad \Leftarrow \quad \boldsymbol{\xi} = (\xi_1, \xi_2)$

Collocation point x: $\quad z_R^x = x_1 + \mu_R x_2 \quad \Leftarrow \quad \mathbf{x} = (x_1, x_2)$

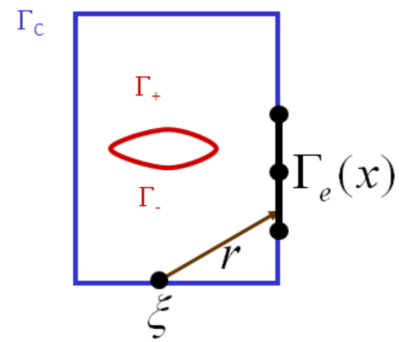

$$c_{IJ} u_J(\boldsymbol{\xi}) + \int_\Gamma p_{IJ}^* u_J \, d\Gamma(\mathbf{x}) = \int_\Gamma u_{IJ}^* p_J \, d\Gamma(\mathbf{x})$$

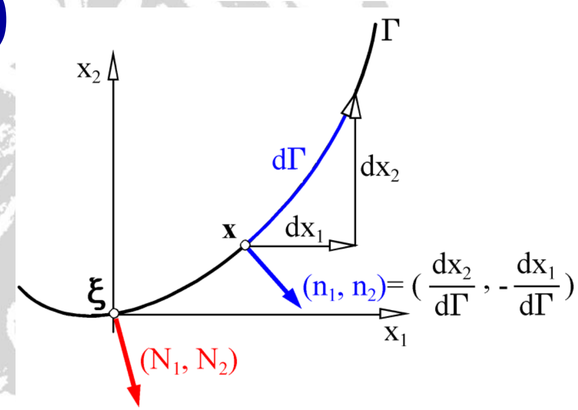

Anisotropic (elastic): Eshelby et al. (1953)

Piezoelectric: Barnett & Lothe (1975)

MEE: Liu et al. (2001)

Evaluation of Strongly Singular and Hypersingular Integrals

Regularization technique follows the works by García-Sánchez et al. (EABE2004, C&S2005, TAFM2008). This approach is valid for any of the 2-D fundamental solutions derived by Stroh's formalism and has no restrictions on the type/shape of the boundary elements:

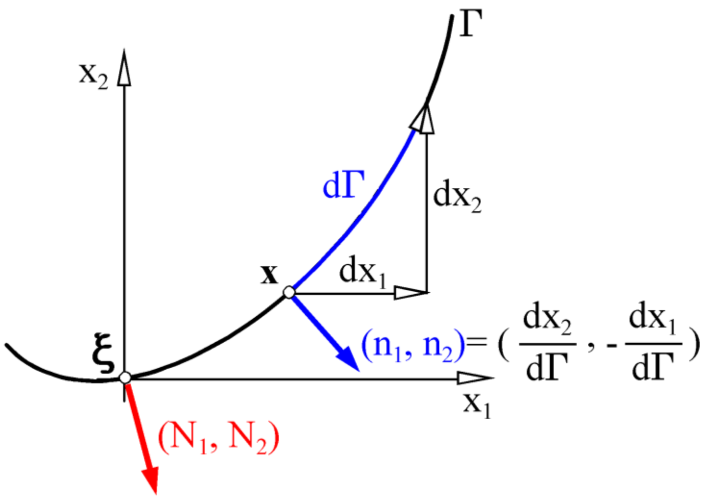

$$p_{IJ}^{*}(\mathbf{x}, \boldsymbol{\xi}) = \frac{1}{\pi} \Re\left[L_{JM} Q_{MI} \frac{\mu_M n_1 - n_2}{z_M^x - z_M^{\xi}} \right]$$

CHANGE OF VARIABLES

$$\chi_R = z_R^x - z_R^{\xi} = (x_1 - \xi_1) + \mu_R (x_2 - \xi_2)$$

THE JACOBIAN IS BUILT-IN THE FUNDAMENTAL SOLUTION

$$\frac{d\chi_R}{d\Gamma} = \frac{d\chi_R}{dx_1}\frac{dx_1}{d\Gamma} + \frac{d\chi_R}{dx_2}\frac{dx_2}{d\Gamma} = -n_2 + \mu_R n_1$$

For instance, for the hypersingular integrations:

$$s_{rIJ}^{*} \approx o\left[\frac{1}{(z^{x}-z^{\xi})^{2}}\right]$$

$$\frac{d\chi_R}{d\Gamma} = \frac{d\chi_R}{dx_1}\frac{dx_1}{d\Gamma} + \frac{d\chi_R}{dx_2}\frac{dx_2}{d\Gamma} = -n_2 + \mu_R n_1$$

$$I''_R = \int_{\Gamma_e} (\mu_R n_1 - n_2)\frac{1}{\chi_R^2}\phi_q d\Gamma$$

$$\phi_q(\chi_R) \approx \phi_q(\chi_R = 0) + \left.\frac{d\phi_q}{d\chi_R}\right|_{\chi_R=0} \cdot \chi_R$$
$$\approx \phi_{q0} + \phi'_{q0} \cdot \chi_R$$

$$I''_R = \underbrace{\int_{\Gamma_e} \frac{1}{\chi_R^2}(\phi_q - \phi_{q0} - \phi'_{q0}\cdot\chi_R)d\chi_R}_{\text{Regular}} + \phi_{q0}\underbrace{\int_{\Gamma_e}\frac{1}{\chi_R^2}d\chi_R}_{\text{Analytic}} + \phi'_{q0}\underbrace{\int_{\Gamma_e}\frac{1}{\chi_R}d\chi_R}_{\text{Analytic}}$$

Evaluation of fracture parameters by extrapolation:

$$\Delta u \rightarrow K_{*} f_{u}(\theta, \mu_R)\sqrt{r}$$

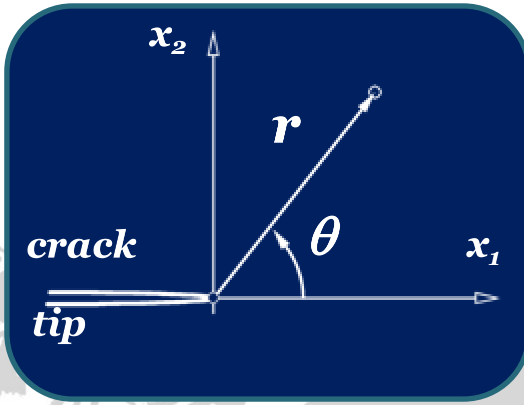

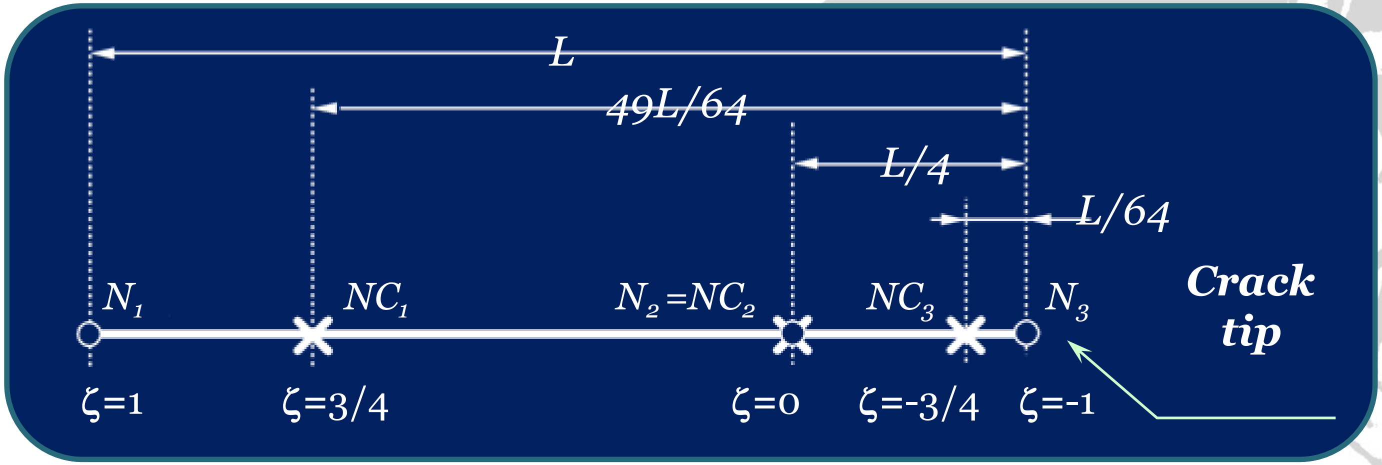

$$\zeta = 2\sqrt{\frac{r}{L}} - 1$$

at NC3

$$\mathbf{K} = \begin{pmatrix} K_{II} \\ K_{I} \\ K_{D} \\ K_{B} \end{pmatrix} = \sqrt{\frac{\pi}{8r}}\,\mathbf{H}^{-1}\begin{pmatrix} \Delta u_1 \\ \Delta u_2 \\ \Delta\phi \\ \Delta\varphi \end{pmatrix}$$

$$\rightarrow \quad G = \frac{1}{2}\mathbf{K}^{T}\,\mathbf{H}\,\mathbf{K}$$

Some results: BEM vs FEM & Experimental Results. Composite material.

ELSEVIER

Available online at www.sciencedirect.com

ScienceDirect

Composite Structures 81 (2007) 614–621

COMPOSITE STRUCTURES

www.elsevier.com/locate/compstruct

Determining stress intensity factors of composites using crack opening displacement

S.H. Ju *, S.H. Liu

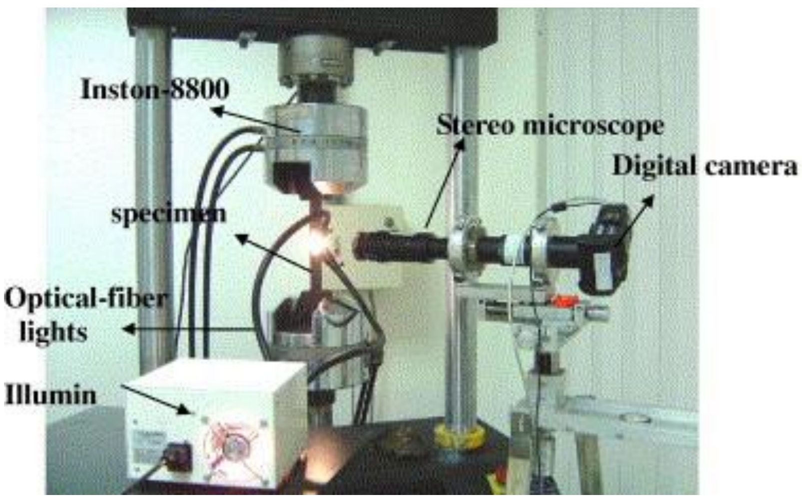

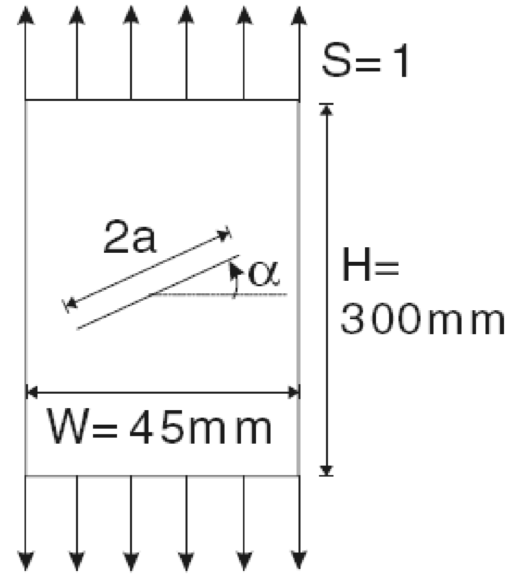

tip. All numerical analysis assume linear-elastic and plane-stress conditions. The applied stress, S, in each case is unity and the material properties are $E_{11} = 101$ GPa, $E_{22} = 25$ GPa, $v_{21} = 0.082$ and $G_{12} = 4.2$ Gpa, where fiber axis 1 is parallel to the specimen longitudinal direction and axis 2 is parallel to the transverse direction. As shown in

60° with respect to the horizontal. The material was a $[0_3/90/0_3/90/0_3/90/0_3]$ 12 K-carbon–fiber/epoxy composite.

FEM Mesh
(*classic* FEM, not X-FEM)

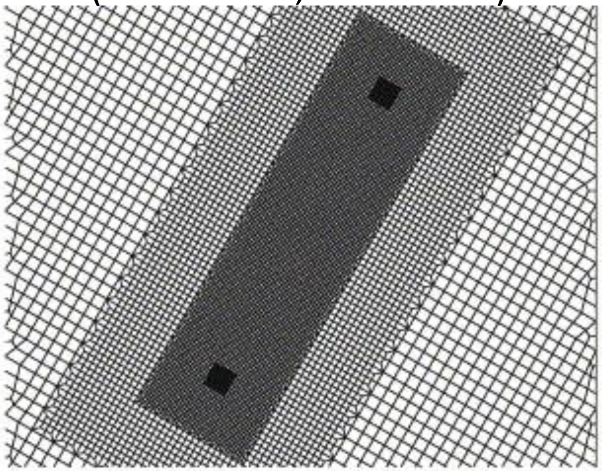

(a) Finite element mesh of near the crack of $\alpha = 60^\circ$ and $2a/W = 0.556$

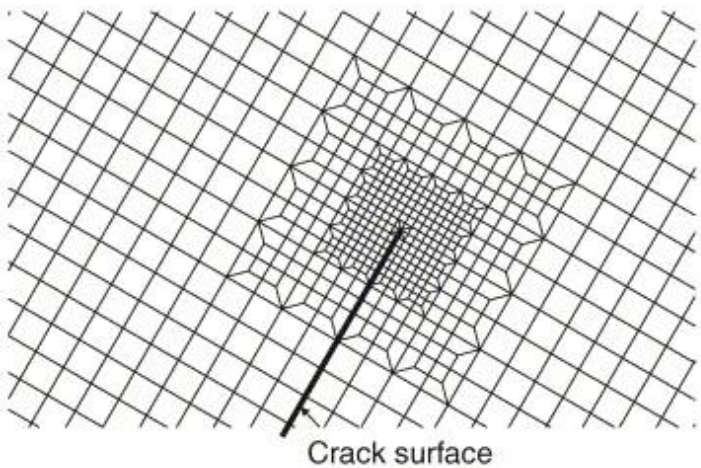

(b) Finite element mesh very near the upper right crack tip

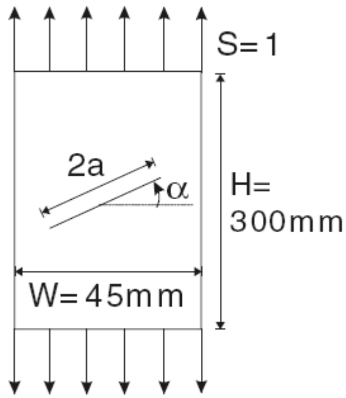

BEM Mesh

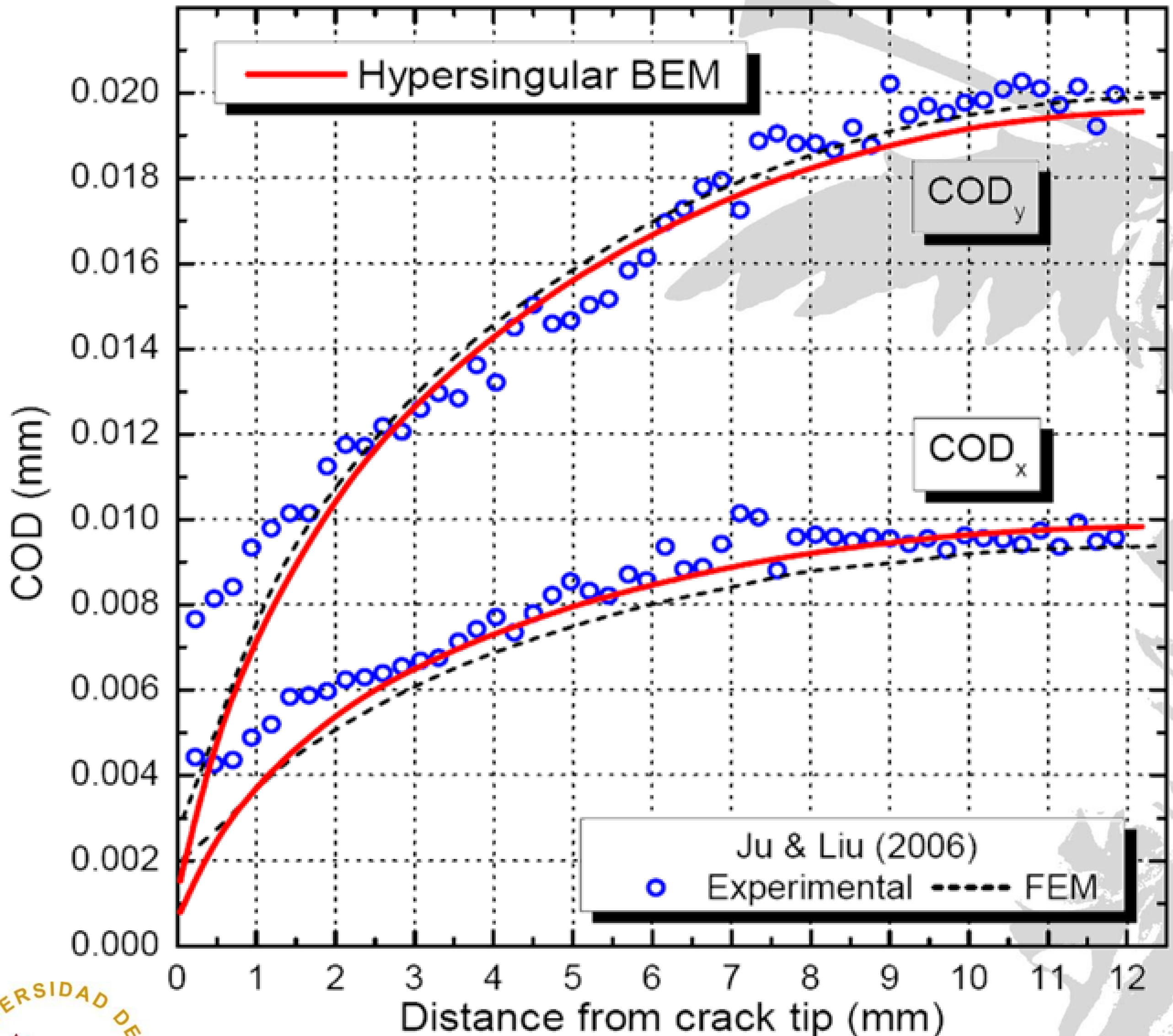
Hypersingular BEM
COD$_y$
COD$_x$
Ju & Liu (2006)
Experimental
FEM
COD (mm)
0.000
0.002
0.004
0.006
0.008
0.010
0.012
0.014
0.016
0.018
0.020
0
1
2
3
4
5
6
7
8
9
10
11
12
Distance from crack tip (mm)

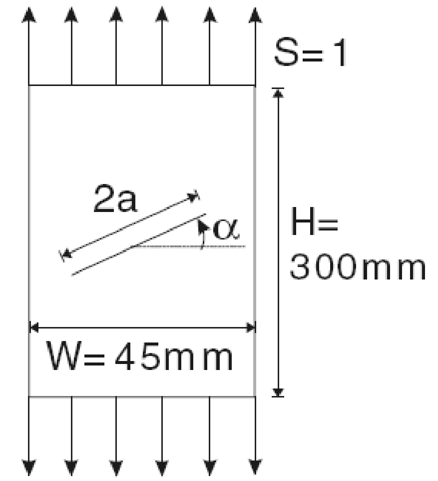
S=1
2a
α
H=
300mm
W=45mm

Some results: BEM vs FEM & Analytic. Piezoelectric material.

Arch Appl Mech (2006) 76: 725–745
DOI 10.1007/s00419-006-0059-z

ORIGINAL

MEF

M. Kuna

Finite element analyses of cracks in piezoelectric structures: a survey

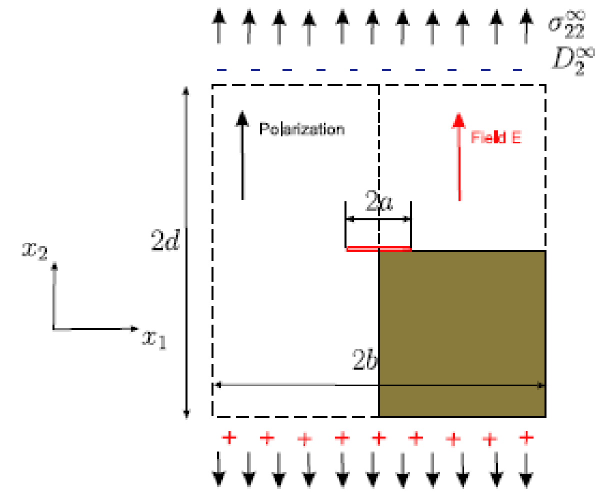

Fig. 9 Griffith crack under remote electromechanical loading

barium titanate ($BaTiO_3$)

	Impermeable $\kappa_C \to 0$
K_I [MPa$\sqrt{m}$] exact	3.545
K_I (CTE) error	1.98%
K_I (MCCI) error	0.68%
K_{IV}[Cm$^{-\frac{3}{2}}$] exact	3.545E-03
K_{IV} (CTE) error	0.85%
K_{IV} (MCCI) error	0.37%

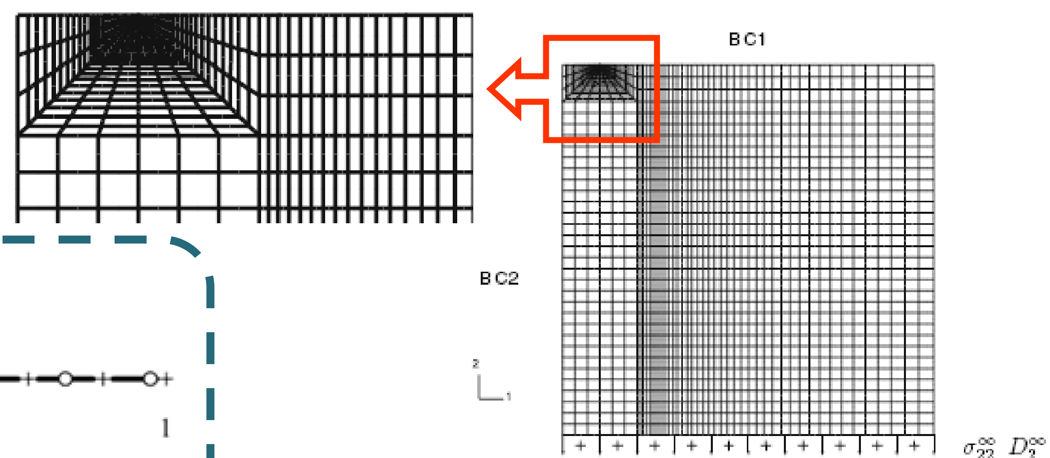

Fig. 10 FEM model and boundary conditions for Griffith crack

BEM

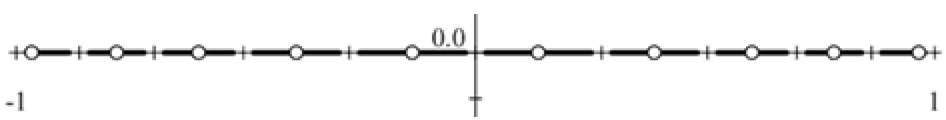

error < 0.1 %

Some results: BEM vs Analytic. MEE material.

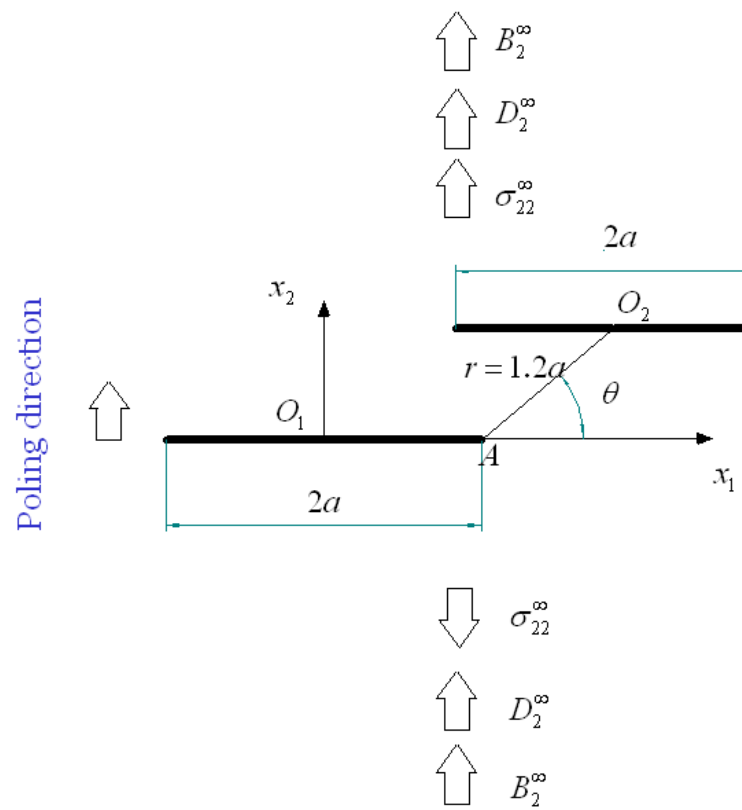

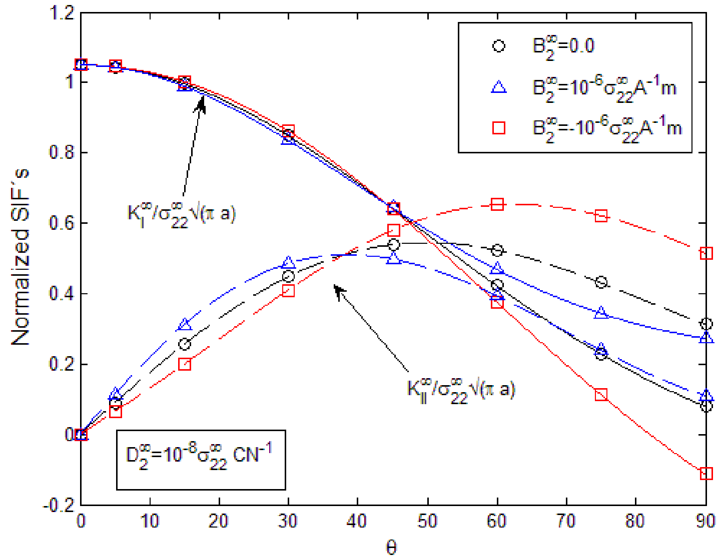

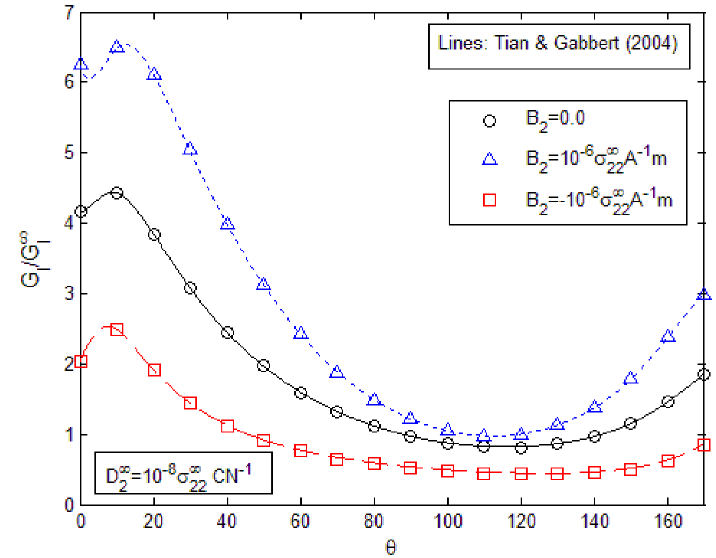

$BaTiO_3$

50%

$CoFe_2O_4$

What about dynamics?

For instance, in the frequency domain, the fundamental solution is obtained as:

$$u^*_{IJ}(\mathbf{x},\xi,\omega)=\frac{1}{8\pi^2}\int_{|\boldsymbol{\eta}|=1}\frac{\gamma^m_{IJ}}{\rho c^2_m}\underbrace{\Phi\left(k_m(\omega)|\boldsymbol{\eta}\cdot(\mathbf{x}-\xi)|\right)}dS(\boldsymbol{\eta})$$

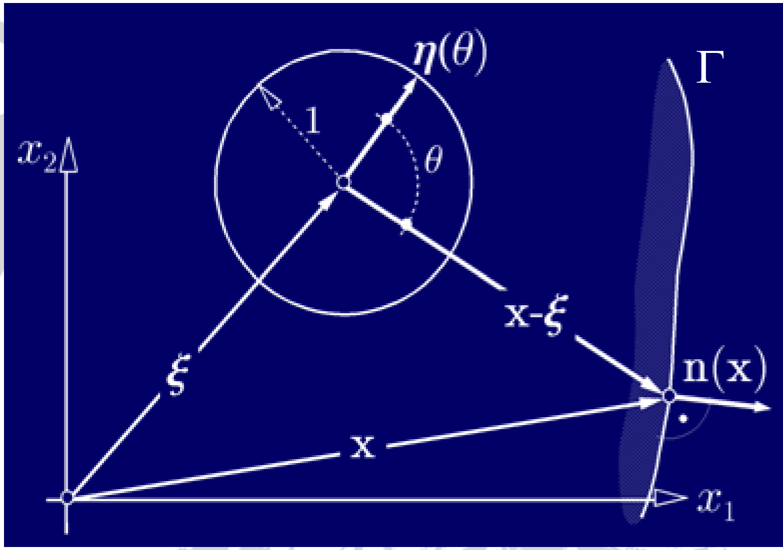

$$\underbrace{\frac{1}{8\pi^2}\int_{|\boldsymbol{\eta}|=1}\frac{\gamma^m_{IJ}}{\rho c^2_m E^m_{qq}}\overbrace{\left[\Phi\left(k_m(\omega)|\boldsymbol{\eta}\cdot(\mathbf{x}-\xi)|\right)+2\ln|\boldsymbol{\eta}\cdot(\mathbf{x}-\xi)|\right]}dS(\boldsymbol{\eta})}_{\text{regular: } u^{*R}_{IJ}(\mathbf{x},\xi,\omega)}-\underbrace{\frac{1}{8\pi^2}\int_{|\boldsymbol{\eta}|=1}\frac{\gamma^m_{IJ}}{\rho c^2_m E^m_{qq}}2\ln|\boldsymbol{\eta}\cdot(\mathbf{x}-\xi)|dS(\boldsymbol{\eta})}_{\text{singular (statics): } u^{*S}_{IJ}(\mathbf{x},\xi)}$$

regular: $u^{*R}_{IJ}(\mathbf{x},\xi,\omega)$

singular: (statics) $u^{*S}_{IJ}(\mathbf{x},\xi)$

Anisotropic: Wang & Achenbach (1995)

Piezoelectric: Denda et al. (2004)

MEE: Rojas-Díaz et al. (2008)

$$\boxed{u^*_{IJ}(\mathbf{x},\xi,\omega)=u^{*S}_{IJ}(\mathbf{x},\xi)+u^{*R}_{IJ}(\mathbf{x},\xi,\omega)}$$

Some dynamic results: Combined magneto-electro-mechanical impacts.

Curved crack in infinite MEE domain

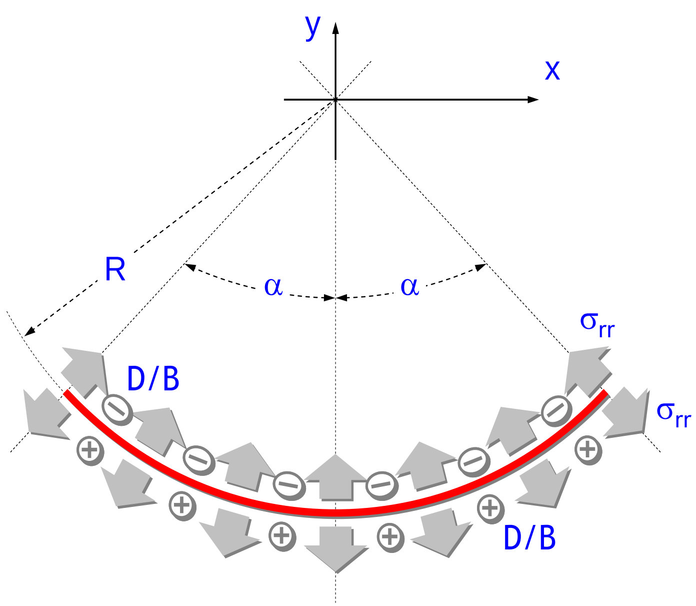

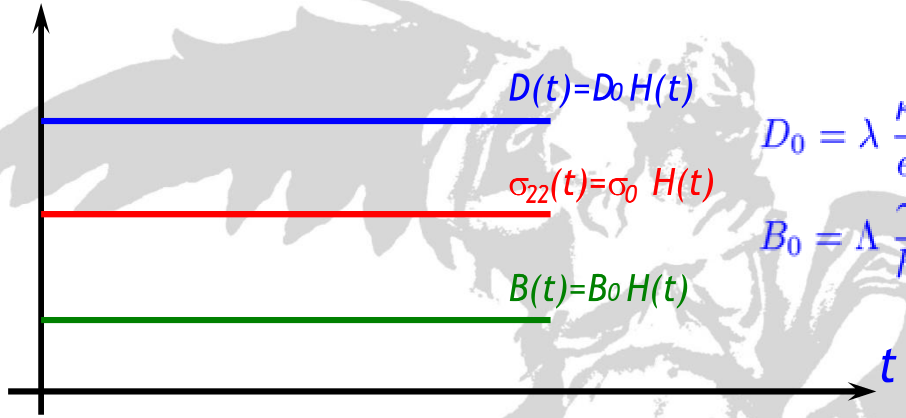

$$D_0 = \lambda \frac{\kappa_{22}}{e_{22}} \sigma_0$$

$$B_0 = \Lambda \frac{\gamma_{22}}{h_{22}} \sigma_0$$

$BaTiO_3$

50%

$CoFe_2O_4$

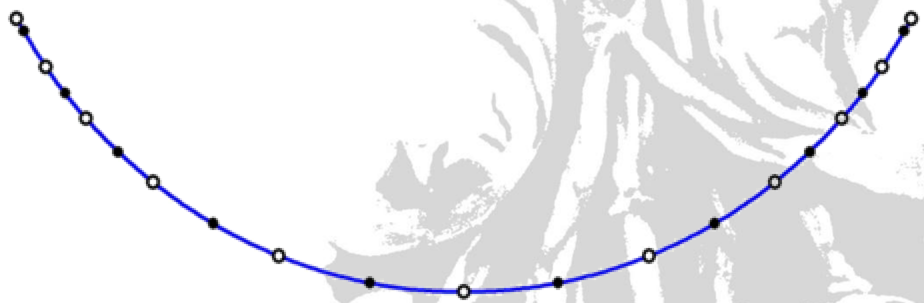

10 discontinuous quadratic elements for the crack (8 + 2 QP)

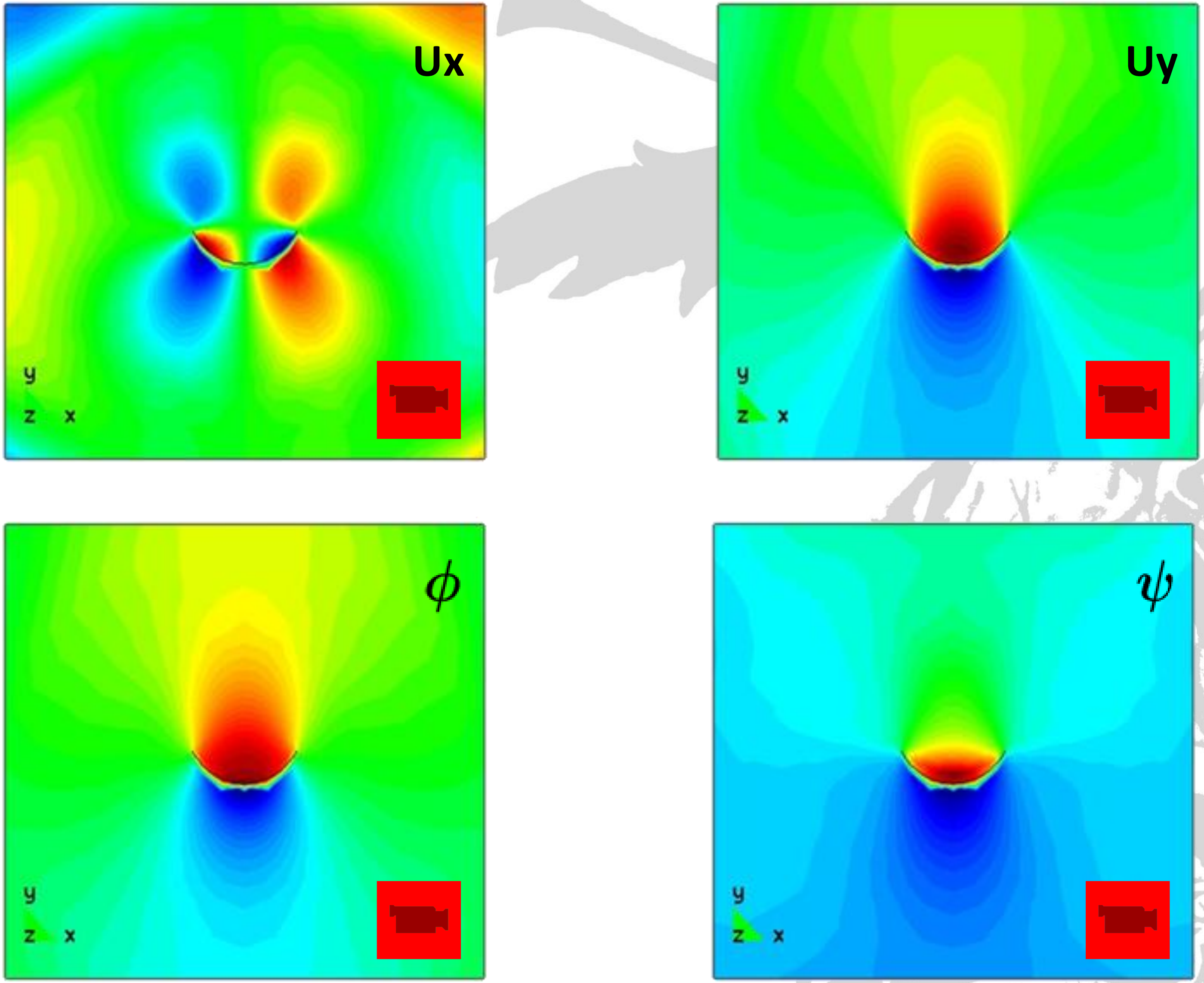
Ux
y
z x
Uy
y
z x
ϕ
y
z x
ψ
y
z x

Some dynamic results: Finite cracked MEE plate under combined magneto-electro-mechanical impacts.

$BaTiO_3$ 50% $CoFe_2O_4$

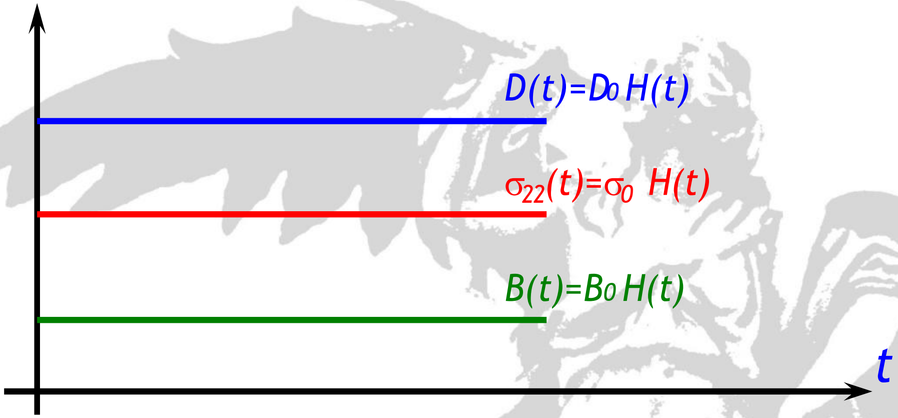

$$\kappa = \frac{e_{22}}{\varepsilon_{22}}\frac{D_0}{\sigma_0}, \quad \chi = \frac{h_{22}}{\gamma_{22}}\frac{B_0}{\sigma_0}$$

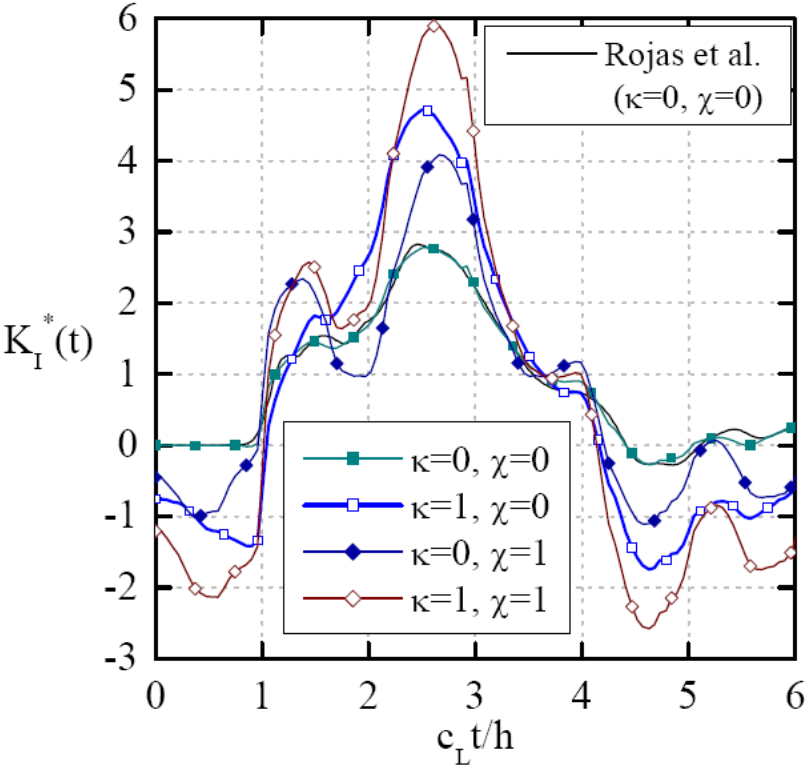

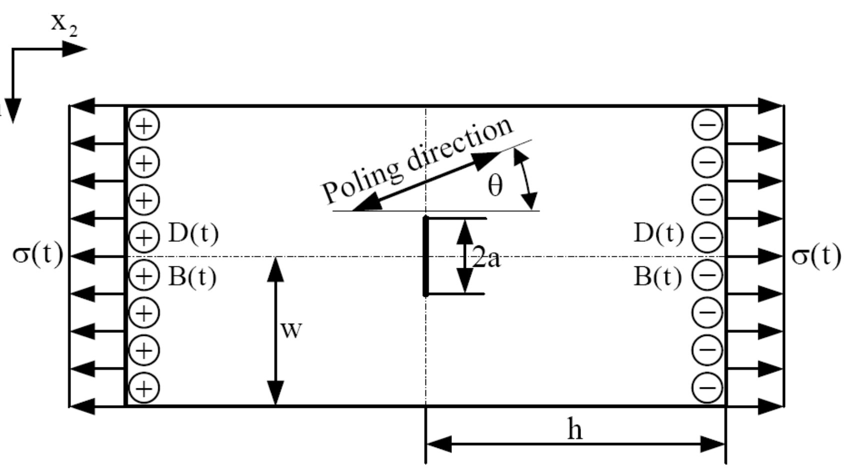

Concluding remarks

✓BEM works for fracture applications!!, leading to accurate evaluation of the relevant fracture parameters

Some additional issues

❖ Realistic boundary conditions

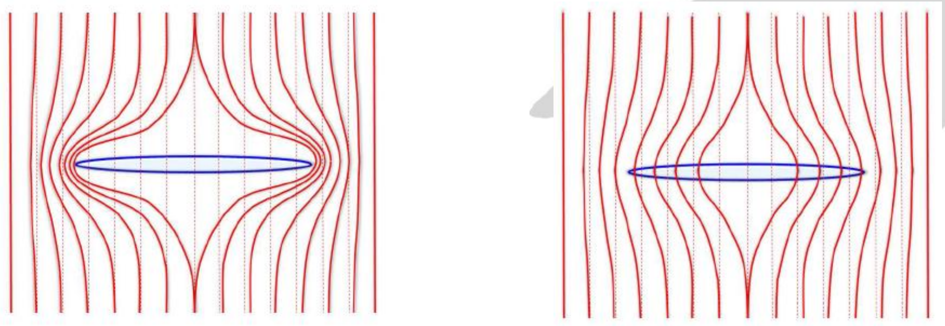

❖ Include other relevant variables (T…) and material nonlinearities

❖ Develop adequate fracture criteria for multifield materials

❖ Improve fundamental solutions

❖ and much more…

Thanks for your attention!!

andres@us.es

Some references of our group's work:

Wünsche, M., García-Sánchez, F., Sáez, A., Zhang, Ch.
A 2D time-domain collocation-Galerkin BEM for dynamic crack analysis in piezoelectric solids
(2010) Engineering Analysis with Boundary Elements, 34 (4), pp. 377-387.

Rojas-Díaz, R., García-Sánchez, F., Sáez, A.
Analysis of cracked magnetoelectroelastic composites under time-harmonic loading
(2010) International Journal of Solids and Structures, 47 (1), pp. 71-80.

Rojas-Díaz, R., García-Sánchez, F., Sáez, A., Zhang, Ch.
Dynamic crack interactions in magnetoelectroelastic composite materials
(2009) International Journal of Fracture, 157 (1-2), pp. 119-130.

García-Sánchez, F., Zhang, C., Sáez, A.
2-D transient dynamic analysis of cracked piezoelectric solids by a time-domain BEM
(2008) Computer Methods in Applied Mechanics and Engineering, 197 (33-40), pp. 3108-3121.

Rojas-Díaz, R., Sáez, A., García-Sánchez, F., Zhang, C.
Time-harmonic Green's functions for anisotropic magnetoelectroelasticity
(2008) International Journal of Solids and Structures, 45 (1), pp. 144-158.

García-Sánchez, F., Rojas-Díaz, R., Sáez, A., Zhang, Ch.
Fracture of magnetoelectroelastic composite materials using boundary element method (BEM)
(2007) Theoretical and Applied Fracture Mechanics, 47 (3), pp. 192-204.

Sáez, A., García-Sánchez, F., Domínguez, J.
Hypersingular BEM for dynamic fracture in 2-D piezoelectric solids
(2006) Computer Methods in Applied Mechanics and Engineering, 196 (1-3), pp. 235-246.

Some references of our group's work:

García-Sánchez, F., Sáez, A., Domínguez, J.
Two-dimensional time-harmonic BEM for cracked anisotropic solids
(2006) Engineering Analysis with Boundary Elements, 30 (2), pp. 88-99.

García-Sánchez, F., Sáez, A., Domínguez, J.
Anisotropic and piezoelectric materials fracture analysis by BEM
(2005) Computers and Structures, 83 (10-11 SPEC. ISS.), pp. 804-820.

García, F., Sáez, A., Domínguez, J.
Traction boundary elements for cracks in anisotropic solids
(2004) Engineering Analysis with Boundary Elements, 28 (6), pp. 667-676.

Sáez, A., Domínguez, J.
Dynamic crack problems in three-dimensional transversely isotropic solids
(2001) Engineering Analysis with Boundary Elements, 25 (3), pp. 203-210.

Sáez, A., Domínguez, J.
Far field dynamic Green's functions for BEM in transversely isotropic solids
(2000) Wave Motion, 32 (2), pp. 113-123.

Sáez, A., Ariza, M.P., Domínguez, J.
Three-dimensional fracture analysis in transversely isotropic solids
(1997) Engineering Analysis with Boundary Elements, 20 (4), pp. 287-298.